

Optical Transitions in Silica Glass During Heavy Ion Implantation

Oleg A. Plaksin^{1,2}, Nariaki Okubo³, Yoshihiko Takeda¹, Hiroshi Amekura¹,
Kenichiro Kono¹, Naoki Umeda³ and Naoki Kishimoto¹

¹Nanomaterials Laboratory, National Institute for Materials Science, Tsukuba, Ibaraki 305-0003, Japan

Fax: 81-298-59-5010, e-mail: plax@mail.ru

²SSC RF – Institute of Physics and Power Engineering, Obninsk, 249033, Russia

³University of Tsukuba, Tsukuba, Ibaraki 305-8573, Japan

Metal nanoparticles fabricated by heavy-ion implantation of insulators are promising for ultra-fast optical devices. Spectra of optical transmission and light emission of silica glass in the visible region were measured during implantation of 3 MeV Cu²⁺ ions. Three absorption bands contribute to the spectra: transient defect absorption at 2.34 eV, a surface plasmon resonance (SPR) peak at 2.21 eV and a tail of residual defect absorption in the range of the photon energy from 2.2 to 2.6 eV. Three bands contribute to the spectra of light emission: a tail of oxygen-deficient center band, the band of Cu⁺ ion at 2.27 eV and the band of non-bridging oxygen hole center at 1.9 eV. The Cu⁺ ion band, which intensity is proportional to Cu solute concentration, appears around 10¹⁴ ions/cm². The SPR peak appears at 3.3×10¹⁶ ions/cm², corresponding to the onset of precipitation. At fluences higher than 4.5×10¹⁶ ions/cm², the growth of nanoparticles predominates, and the fluence dependence of SPR peak is linear. At the stage of nanoparticle growth, the Cu solute concentration does not change.

Key words: ion implantation, metal nanoparticles, silica glass, in-situ measurements, optical properties

1. INTRODUCTION

Silica glasses containing metal nanoparticles fabricated by heavy-ion implantation are promising materials for ultra-fast optical devices in the THz region and magneto-optical applications [1, 2]. Ion implantation provides good controllability, though nanoparticle formation is conditioned by various competitive processes induced by the implantation, either by atomic collisions or electronic excitation [3]. Swift-heavy-ion implantation, i.e. the implantation of ions in the MeV range of kinetic energy, has the advantage of a strongly reduced surface recession by sputtering, as compared to ions in the keV range [4].

An enhanced energy deposition during swift-heavy-ion irradiation limits allowable ion fluxes, in this way increasing the irradiation time necessary for the production of nanoparticles. Recently, a method of enhanced nanoparticle formation in silica glass under co-irradiation by laser and heavy ions has been developed [5]. The co-irradiation also improves the optical quality of the implanted silica glass, namely, it decreases the defect absorption [6].

For understanding the mechanisms of nanoparticle formation and co-irradiation, in-situ measurements of radiation-induced optical properties are necessary. This study focuses on time-resolved measurements of the optical properties of radiation-resistant silica glass during swift-heavy-ion implantation.

2. EXPERIMENTAL

Disk-shaped specimens of KU-1 silica glass

(OH concentration 800 ppm) were irradiated by 3 MeV Cu²⁺ ions at a constant current density of 2-10 μA/cm² (6×10¹² - 3×10¹³ ions/cm²s) up to a fluence of 1×10¹⁷ ions/cm². Time-resolved optical devices based on fast-response intensified CCD cameras collected spectra of optical transmission and ion-induced light emission (IILE) in the wavelength range from 470 to 720 nm. To ensure the efficient heat removal from a substrate under irradiation, the following arrangement was chosen for the measurements of optical transmission. The specimens were placed in a massive sample holder made of copper and covered by a copper mask with a hole of 12 mm in diameter. The Xe lamp illuminated the irradiated surfaces of the specimens. A gold film was deposited onto the backside of the specimens to obtain much higher reflection as compared to that of irradiated surfaces.

During the experiments we interrupted the ion irradiation several times to be able to compare the spectra of optical transmission during and after irradiation at the same fluence (Fig.1). Switching off and subsequent switching on the irradiation resulted in reversible changes of the optical spectra. From the spectra measured, the optical absorption was derived. To calculate the absorption we also used data on optical reflection of uncoated specimen measured both after irradiation by using a dual beam spectrometer and during implantation.

Absorption bands contributing the optical spectra were separated by means of Alentsov's method [7] valid for non-Gaussian shapes of optical bands. The method is based on a linear

combination of two or more spectra obtained at slightly different conditions. The different conditions are necessary to change contributions from bands to spectra. In general, N spectra are used to separate N bands, assuming that the contributions from the bands are independent. To separate bands, we used the spectra measured at different ion fluences, anticipating different fluence dependencies of the bands.

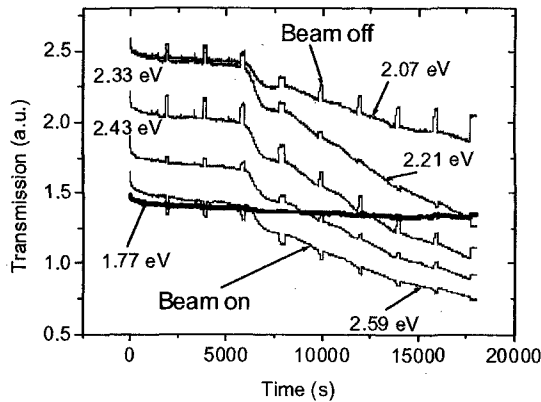


Fig.1. Time dependencies of optical transmission (current density of $2 \mu\text{A}/\text{cm}^2$).

3. RESULTS AND DISCUSSION

Figure 2 shows optical absorption spectra as measured just before (beam on) and after (beam off) the interruption of the Cu implantation at fluences from 1.1×10^{16} to 1×10^{17} ions/cm². At fluences higher than 4×10^{16} ions/cm², the optical spectra are completely different from those at lower fluences. Peaks typical for surface plasmon resonance (SPR) at 2.21 eV in the beam-off spectra indicate the formation and growth of Cu nanoparticles. No SPR peak is observed at low fluences. Tentatively, we associated the absorption at low fluences with defect absorption.

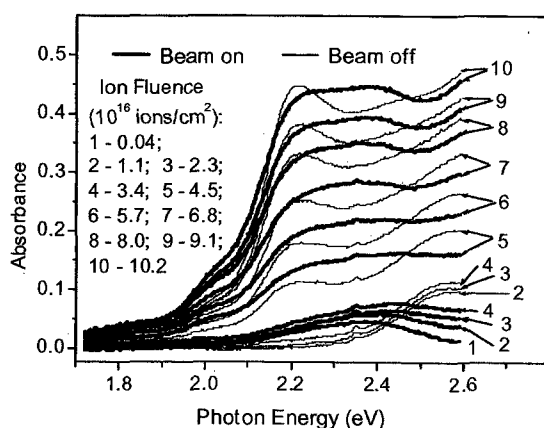


Fig.2. Absorption spectra of Cu implanted silica glass.

Spectra of residual defect absorption (RDA) that were measured after irradiation differ from those measured during irradiation (Fig.2, sets 1-4). The shapes of the spectra remain almost the

same with increasing fluence, except in the range from 2.4 to 2.6 eV where a slight change of absorption is observed during irradiation. Figure 3a shows that the defect absorption during irradiation comprises two bands: a weak band with the same shape as RDA and transient defect absorption (TDA) with a maximum at 2.34 eV. The latter has the same shape as the band at 4×10^{14} ions/cm² (Fig.2, curve 1). In this particular case, we used the beam-on spectra at 2.3×10^{16} and 3.4×10^{16} ions/cm² to separate the bands. By this example, it is shown that the consistent results are obtained by the method of linear combination of bands.

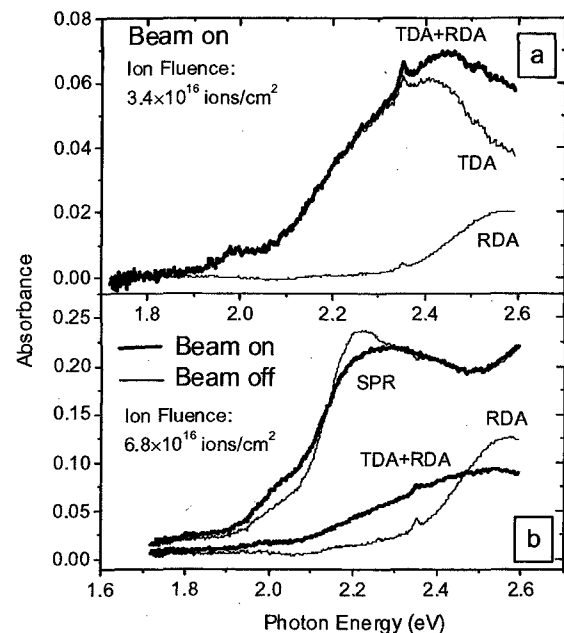


Fig.3 Bands contributing the optical absorption of Cu implanted silica glass.

The absorption measured during irradiation quickly increases at the onset of irradiation. However, the TDA is almost constant at fluences higher than 5×10^{14} ions/cm² (Fig.4). The TDA may contribute to (a) the enhanced nanoparticle formation during the co-irradiation by the 532 nm laser and 3 MeV Cu²⁺ ions [5] and (b) the decrease of defect absorption of silica glass under the co-irradiation [6]. During co-irradiation, the laser processing is highly efficient. Its mean energy deposition rate of 10^4 Gy/s is calculated from the mean laser power and TDA, whereas ion irradiation is characterized by a dose rate of 10^6 - 10^7 Gy/s.

The origin of TDA and RDA is unknown. They are not caused by Cu solutes because the only known absorption band of Cu⁺ ions in silica glass is reported to be at 4.6 eV [8]. To our knowledge, they have never been observed in undoped or OH-doped silica glasses, though an absorption band in the same range as that of TDA was observed in silica-core optical fibers during neutron and gamma irradiation [9]. The closest to TDA is the position of a band at 2.25 eV reported

in the paper [10] for gamma-irradiated silica fibers and ascribed to traps of electrons. Probably, the origin of TDA is also associated with electronic excitation and charge carrier evolution during Cu implantation.

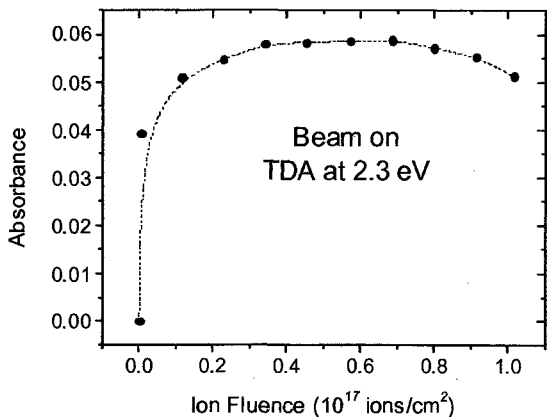


Fig.4. Fluence dependence of TDA at 2.3 eV.

At fluences higher than $3.4 \cdot 10^{16}$ ions/cm², both the SPR peak and the defect absorption contribute to the optical spectra. The bands separated from each other are presented in Fig.3b. After irradiation, the defect absorption band is of the same shape as RDA at low fluences, though no pre-assumption on band shapes was done when Alentsov's method of band separation was used. As it has been mentioned already, the contribution from the TDA is almost constant at high fluences. The TDA and a change of the SPR peak strongly contribute to the total transient absorption obtained as a difference in absorption during and after irradiation. Upon switching the ion beam on, the change of RDA shows up as a decrease of absorbance in the range from 2.4 to 2.6 eV (Fig.1, curve for 2.59 eV).

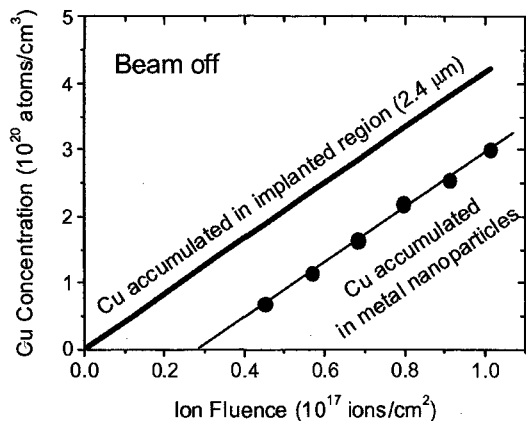


Fig.5. Fluence dependence of the concentration of Cu accumulated in metal nanoparticles.

The SPR peaks, both during and after irradiation, have linear fluence dependencies for fluences from $3.4 \cdot 10^{16}$ to $1 \cdot 10^{17}$ ions/cm²; and the ratio of the SPR peaks is almost constant with increasing the fluence. Assuming proportionality

between the absorption cross-section and the volume of the nanoparticles [11], this behavior corresponds to a linear dependence of the number of Cu atoms accumulated in nanoparticles on ion fluence. The dependence of the SPR peak after irradiation on the atomic fraction of Cu in the implanted region was evaluated by using the Maxwell-Garnett theory. Fig.5 illustrates the fluence dependencies of (a) the amount of Cu accumulated in metal nanoparticles and (b) the Cu concentration of implanted region, the former being parallel to the latter. That is, the concentration of Cu in the solute and other states (possibly Cu₂O) is constant during the growth of metal nanoparticles, and all of the Cu atoms implanted during that period are accumulated as in the nanoparticles.

The linear trend lines of the fluence dependencies of the SPR peaks (see Fig.4) intersect the axis of fluence at $3 \cdot 10^{16}$ ions/cm², for as well during as after irradiation. However, during implantation, the SPR peak becomes visible at a slightly higher fluence of $3.3 \cdot 10^{16}$ ions/cm², corresponding to the onset of precipitation of Cu atoms. The SPR peak quickly increases in a narrow range of fluences. Then the linear fluence dependence is observed. That is, the nanoparticles appear from a super saturated region. The precipitation and the growth occur as well distinguishable stages of nanoparticle formation.

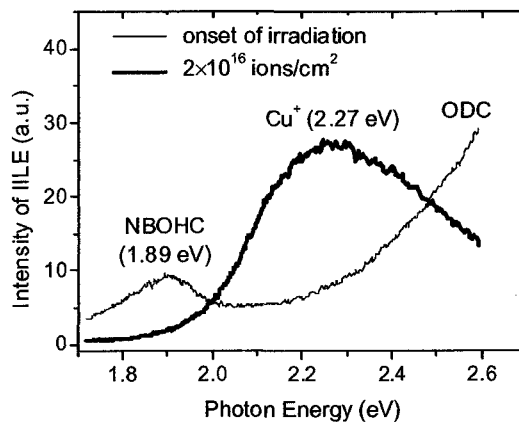
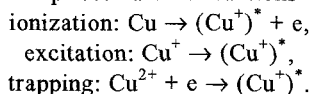


Fig.6. Spectra of IILE at a current density of 5 $\mu\text{A}/\text{cm}^2$.

Spectra of IILE comprised contributions from three bands (Fig.6): the band of Cu⁺ solutes at 2.27 eV [8], the band of non-bridging oxygen hole center (NBOHC) at 1.9 eV [12] and a tail of oxygen-deficient center (ODC) band usually peaked at 4.3-4.4 eV [12]. The fluence dependencies of the separated bands are shown in Fig.7. The bands of intrinsic defects quickly decrease at the onset of irradiation and become invisible at a fluence of $5 \cdot 10^{14}$ ions/cm². No Cu⁺-band is observed at the onset of irradiation, followed by the appearance of the band, its growth and saturation at a fluence about $3\text{-}4 \cdot 10^{16}$ ions/cm².

The intensity of the Cu^+ -band of IILE is proportional to the rate of production of excited $(\text{Cu}^+)^*$ ions. The ionization-induced production of $(\text{Cu}^+)^*$ ions comprises various reactions



However, the electronic equilibrium of the trap subsystem is reached in a few seconds after the onset of irradiation, because of the high ionizing dose rate about 10^7 Gy/s [13]. It is consistent with the time dependencies of TDA and IILE bands of intrinsic defects, which presented in Figs.4 and 7 respectively. Therefore, the IILE intensity is proportional to the Cu solute concentration during implantation. Accordingly, the fluence dependence of Cu^+ -band of IILE represents (a) the accumulation of Cu solutes preceding the nanoparticle formation and (b) no change of Cu solute concentration during nanoparticle growth.

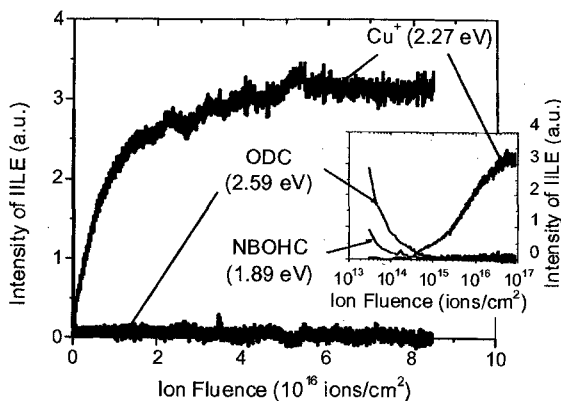


Fig.7. Fluence dependencies of IILE bands at a current density of $5 \mu\text{A}/\text{cm}^2$.

4. CONCLUSION

Spectra of the optical transmission and IILE of silica glass were measured during implantation of 3 MeV Cu ions at a constant current density of $2\text{--}10 \mu\text{A}/\text{cm}^2$ up to a fluence of 1×10^{17} ions/ cm^2 . The results can be summarized as follows:

- 1) Three absorption bands contribute to optical transmission during and after irradiation: transient absorption (TDA) at 2.34 eV, a surface plasmon resonance (SPR) peak at 2.21 eV and a tail of residual absorption (RDA) in the range of the photon energy from 2.2 to 2.6 eV.
- 2) Three bands contribute to the IILE spectra: a tail of ODC band, the band of Cu^+ ions at 2.27 eV and the band of NBOHC at 1.9 eV. The Cu^+ ion band appears at a fluence of 10^{14} ions/ cm^2 .
- 3) Intrinsic defects of silica glass contribute to the optical absorption and IILE at the onset of irradiation only. At fluences higher than 5×10^{14} ions/ cm^2 , the optical properties change because of the accumulation of Cu solutes and the metal nanoparticle formation.
- 4) The TDA provides a means for selective electronic excitation by a laser during implantation. The selective excitation causes a high efficiency of laser radiation (dose rate 10^4

Gy/s) for nanoparticle formation during ion irradiation ($10^6\text{--}10^7$ Gy/s).

5) The precipitation and the growth of clusters are well distinguishable stages of the nanoparticle formation. The SPR peak appears at a fluence of 3.3×10^{16} ions/ cm^2 , corresponding to the onset of precipitation. At fluences higher than 4.5×10^{16} ions/ cm^2 , the growth of nanoparticles predominates, and the fluence dependence of the SPR peak is linear. At the stage of nanoparticle growth, the Cu solute concentration does not change.

ACKNOWLEDGEMENT

A part of this study was financially supported by the Budget for Nuclear Research of the MEXT, based on the screening and counseling by the Atomic Energy Commission.

REFERENCES

- [1] R.F. Haglund, *Materials Science and Engineering A*, 253, 275-83 (1998).
- [2] Y. Takeda, C.G. Lee, V.V. Bandourko, N. Kishimoto, *Materials Transactions*, 43 (2002) 1057-60.
- [3] E. Valentin, H. Bernas, C. Ricolleau, F. Creuzet, *Physical Review Letters*, 86, 99-102 (2001).
- [4] Y. Takeda, C.G. Lee, N. Kishimoto, *Nucl. Instrum. & Methods B*, 191, 422-27 (2002).
- [5] N. Kishimoto, N. Okubo, N. Umeda, Y. Takeda, *Nucl. Instrum. & Methods B*, 191, 115-20 (2002).
- [6] N. Kishimoto, N. Okubo, N. Umeda, Y. Takeda, *Proceedings of SPIE*, 4636, 88-96 (2002).
- [7] M.V. Fock, *Proceedings of the Physical Institute (FIAN)*, 59, 3-13 (1972) (In Russian).
- [8] K. Fukumi, A. Chayahara, K. Ohora, et al, *Nucl. Instrum. & Methods B*, 149, 77-80 (1999).
- [9] T. Kakuta, T. Shikama, T. Nishitani, et al, *Nucl. Instrum. & Methods B*, 307-311, 1277-81 (2002).
- [10] P.V. Chernov, E.M. Dianov, V.N. Karpechev, et al, *Phys. Stat. Sol. B*, 155, 663-75 (1989).
- [11] U. Kreibitz, M. Vollmer, "Optical Properties of Metal Clusters", Ed. by J.P. Toennis, Springer-Verlag, Berlin (1995) p.31.
- [12] L. Skuja, *Journal of Non-Crystalline Solids*, 239, 16-48 (1998).
- [13] O.A. Plaksin, V.A. Stepanov, P.A. Stepanov, P.V. Demenkov, V.M. Chernov, A.O. Krutskikh, *Nucl. Instrum. & Methods B*, 193, 265-70 (2002).

(Received October 9, 2003; Accepted January 20, 2004)